Adsorption of a single polymer chain on a surface: Effects of the potential range

Leonid I. Klushin,[1] Alexey A. Polotsky,[2] Hsiao-Ping Hsu,[3,*] Denis A. Markelov,[2,4] Kurt Binder,[3] and Alexander M. Skvortsov[5,†]

[1]*Department of Physics, American University of Beirut, P. O. Box 11-0236, Beirut 1107 2020, Lebanon*
[2]*Institute of Macromolecular Compounds of Russian Academy of Sciences, Bolshoy pr. 31, 199004 St. Petersburg, Russia*
[3]*Institut für Physik, Johannes Gutenberg-Universität Mainz, Staudinger Weg 7, D-55099 Mainz, Germany*
[4]*St. Petersburg State University, Physical Faculty, Ulyanovskaya ul. 1, 198504 Petrodvorets, St. Petersburg, Russia*
[5]*Chemical-Pharmaceutical Academy, ul. Prof. Popova 14, 197022 St. Petersburg, Russia*

(Received 23 December 2012; published 27 February 2013)

We investigate the effects of the range of adsorption potential on the equilibrium behavior of a single polymer chain end-attached to a solid surface. The exact analytical theory for ideal lattice chains interacting with a planar surface via a box potential of depth U and width W is presented and compared to continuum model results and to Monte Carlo (MC) simulations using the pruned-enriched Rosenbluth method for self-avoiding chains on a simple cubic lattice. We show that the critical value U_c corresponding to the adsorption transition scales as $W^{-1/\nu}$, where the exponent $\nu = 1/2$ for ideal chains and $\nu \approx 3/5$ for self-avoiding walks. Lattice corrections for finite W are incorporated in the analytical prediction of the ideal chain theory $U_c \approx (\frac{\pi^2}{24})(W + 1/2)^{-2}$ and in the best-fit equation for the MC simulation data $U_c = 0.585(W + 1/2)^{-5/3}$. Tail, loop, and train distributions at the critical point are evaluated by MC simulations for $1 \leqslant W \leqslant 10$ and compared to analytical results for ideal chains and with scaling theory predictions. The behavior of a self-avoiding chain is remarkably close to that of an ideal chain in several aspects. We demonstrate that the bound fraction θ and the related properties of finite ideal and self-avoiding chains can be presented in a universal reduced form: $\theta(N,U,W) = \theta(NU_c, U/U_c)$. By utilizing precise estimations of the critical points we investigate the chain length dependence of the ratio of the normal and lateral components of the gyration radius. Contrary to common expectations this ratio attains a limiting universal value $\langle R_{g\perp}^2\rangle/\langle R_{g\parallel}^2\rangle = 0.320 \pm 0.003$ only at $N \sim 5000$. Finite-N corrections for this ratio turn out to be of the opposite sign for $W = 1$ and for $W \geqslant 2$. We also study the N dependence of the apparent crossover exponent $\phi_{\text{eff}}(N)$. Strong corrections to scaling of order $N^{-0.5}$ are observed, and the extrapolated value $\phi = 0.483 \pm 0.003$ is found for all values of W. The strong correction to scaling effects found here explain why for smaller values of N, as used in most previous work, misleadingly large values of $\phi_{\text{eff}}(N)$ were identified as the asymptotic value for the crossover exponent.

DOI: 10.1103/PhysRevE.87.022604 PACS number(s): 36.20.−r, 64.60.−i, 68.47.Pe, 02.70.−c

I. INTRODUCTION

The study of polymer adsorption from a solution onto a solid surface has a long history [1] and is important for many applications such as adhesion, surface coating, wetting, adsorption chromatography, etc. [2]. A fundamental issue is the phase transition associated with the adsorption-desorption transition point of a very long single polymer chain grafted to the surface [3,4]. It is widely believed that generic features of this problem can be elucidated by the study of simple coarse-grained models. The first exact analytical theory of adsorption for an infinitely long single polymer chain was presented in 1965 by Rubin [5] for a random walk on a regular lattice with equal probability of each step in all directions, including back steps (immediate return). Later, different variations of the lattice model of a polymer chain were widely exploited. These included partly or fully directed walk models [6–8], nonrestricted random walks with different statistical weights of kinks [9] (this allowed taking into account the effect of chain stiffness), and restricted random walks where immediate return was forbidden [10] (thus, the excluded volume effects of the nearest-neighbor segments were taken into account). The influence of excluded volume interactions between monomer units on the adsorption behavior and, in particular, on the adsorption-desorption transition point was investigated numerically intensively (see Ref. [11] with references) and by renormalization group methods [4]. A considerable number of works was devoted to the study of regular and statistical (random) copolymer adsorption onto homogeneous solid substrate or onto heterogeneous surface bearing adsorbing and inert sites; see Ref. [12] as an example.

However, some important aspects, such as the precise value of the "crossover exponent" ϕ [4] at the adsorption transition, are still controversial and constitute an important gap in our understanding of this problem.

In many of the cited papers, lattice models of polymer chains were used and the interactions of monomer units with the adsorbing surface was modeled as a square-well potential of a unit width equal to the chain segment size. In other words, the attractive part of the adsorption potential was extended only to the first lattice layer adjacent to the surface.

A considerable advantage of lattice models is the possibility of obtaining analytical expressions for the partition function of infinitely long adsorbed homopolymers and, in certain cases, for heteropolymer chains. Another attractive feature of lattice polymer models is a small number of model parameters involved that describe the model.

*hsu@uni-mainz.de
†astarling@yandex.ru

In coarse-grained off-lattice bead-spring models of a flexible chain, various forms of the effective surface interaction were assumed. As an example, in Refs. [13–15] the surface interaction was specified by a square-well potential. In Refs. [16,17] this potential has a form of Lennard-Jones type with different exponents: 4–10, 3–9, and 1–12. The width of these potentials was never varied. One generally expects that universal properties near the adsorption transition (critical exponents, scaling functions, etc. [4]) should not depend on details of the potential, but this has never been systematically checked.

An analytical theory of polymer adsorption for a continuum ideal chain model was developed by Lépine and Caillé [18] and Eisenriegler *et al.* [19]. In this theory, the monomer-surface potential was replaced by the de Gennes boundary condition [20,21] imposed on the Green's function. Continuum theories were formulated in terms of a phenomenological parameter c (the pseudopotential amplitude), which defines the boundary condition for the diffusion equation describing a Gaussian polymer chain. The interaction parameter c captures both the adsorption and repulsion effects of the real potential and relates them to the structure of a long grafted chain. The main advantage of the continuum theory is that it allows an exact analytical solution for the Green's function of finite chains, yielding their partition function as well as geometric characteristics. There is a rather extensive range of applications of the continuum model to different adsorption problems considered in the literature, especially in liquid chromatography [22] and in colloid science [23]. The availability of closed analytical expressions for the partition functions of ideal lattice and continuum model chains allows a mapping between the lattice adsorption energy parameter and the phenomenological parameter c and provides the latter with a molecular interpretation [24]. This allows us to attribute a molecular physical meaning to the interaction parameter c.

The range of the adsorption interaction in real situations can, indeed, vary from one system to another. One experimental way of changing this range pertains to ionizable polymers where the Debye screening length can be affected by salt concentration. However, adding salt not only changes the potential range but also affects its general shape. One could argue that surface modification with grafted chains used in reverse-phase absorbents is another experimental realization of an effective potential that extends over a range that can be changed from few angstroms to a few nanometers. Currently, the chains used for surface modification are quite short, in the range of C_5–C_{18} with the layer thickness on the order of 1 nm. It was shown that the critical adsorption energy does depend on the molecular mass of the grafted chain of the reverse phase [22]. Recent advances in surface modification by polymer brushes with grafted chains of much larger molecular mass bring potential possibilities of providing attractive potentials extending to tens of nanometers. The focus of our investigation was exactly the effects of the potential width on single-chain adsorption. While for universal properties pertaining to the limit of infinitely long chains such effects are supposed to be nonexistent, we gain insight into their role for chains of finite lengths.

The paper is organized as follows. Section II introduces the lattice and continuum models and lists the main approaches that are valid for finite chains and in the infinite chain limit. Section III describes the results as a function of the potential width at the critical adsorption point for all the models and introduces the scaling laws and the lattice corrections. With the pruned-enriched Rosenbluth method (PERM), the critical point estimation of self-avoiding chains with high precision is demonstrated. Universality of adsorption properties of finite chains is then shown and explained on the basis of the notion of segment renormalization. The tail, loop, and train size distributions at the critical point are evaluated by use of Monte Carlo (MC) simulations for $1 \leqslant W \leqslant 10$ and compared to the analytical results for ideal chains and the predictions of the scaling theory. The length-dependent scaling behavior of the universal ratio between the normal and the lateral components of the gyration radius and the crossover exponent near the adsorption transition are investigated. The correction to scaling is also considered. Section IV presents some remarks on the problems related to the analysis of simulation data in estimating the adsorption critical point and in the evaluation of universal constants associated with critical behavior. We also pose the question of rationalizing the broad range of critical energies found in the literature in view of the effects of the potential width. The appendix provides the details of derivations of the generating functions and the analysis of their singularities.

II. MODEL AND APPROACHES

We consider a polymer chain attached by one end to a planar adsorbing surface and having the other end free. The adsorbing surface interacts with monomer units of the chain via a potential $V(z)$. The surface potential has a square-well shape with the depth U ($U > 0$) and the width W (Fig. 1)

$$V(z) = \begin{cases} -U, & 0 < z \leqslant W \\ 0, & z > W \end{cases}. \tag{1}$$

Here and below we will measure all thermodynamic characteristics in units of temperature $k_B T$.

A. Analytical approach for an ideal chain in the continuum using the quantum-mechanical analogy

For the model of ideal polymer chains (N Kuhn segments of length b are randomly linked [25]) in the continuum, the standard approach exploits the quantum-mechanical analogy and admits the exact solution for the partition function of a polymer chain in an external potential $V(\mathbf{r})$. The partition function of a chain with two ends fixed at the points $\mathbf{r}_0$ and

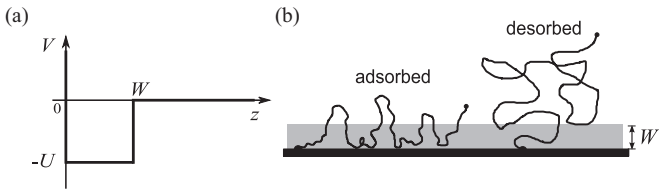

FIG. 1. (a) Square-well adsorption potential and (b) schematic view of end-grafted polymer chain in a finite-range potential well in the adsorbed and desorbed (flower) states.

r (called the Green's function) obeys the following partial differential equation:

$$\frac{\partial G(r_0,r,s)}{\partial s} = \frac{b^2}{6}\frac{\partial^2 G(r_0,r,s)}{\partial r^2} - V(r)G(r_0,r,s), \qquad (2)$$

where b is the Kuhn segment length, Nb is the chain's contour length, s is the continuous monomer index, and **r** is the vector specifying the position of the corresponding segment.

For the continuum chain model the path-integral representation of the partition function leads to an equivalent formulation in terms of a Green's function of a partial differential equation (analog of the Schrödinger propagator). If the partition function is dominated by the ground-state contribution, as in the case for the adsorbed state, the description simplifies dramatically [20,21]. The chemical potential per monomer, μ, is then analogous to the quantum-mechanical energy of the localized ground state and $G(r_0,r,s) = \exp(-\mu s)\psi(r_0)\psi(r)$ is given by the solution of the eigenvalue problem:

$$\left[-\frac{b^2}{6}\frac{d^2}{dz^2} + V(r)\right]\psi = \mu\psi. \qquad (3)$$

For the rectangular potential of Eq. (1) the bound state exists if the potential well is deeper than the critical value,

$$U_c = \frac{\pi^2 b^2}{24W^2}. \qquad (4)$$

The chemical potential is given by

$$\mu = -U + \frac{4}{\pi^2}U_c x^2, \qquad (5)$$

where x is the smallest root of the transcendental equation [26]

$$x\cot x = -\sqrt{\frac{\pi^2}{4}\frac{U}{U_c} - x^2}. \qquad (6)$$

It follows from Eqs. (5) and (6) that $x = x(U/U_c)$, the chemical potential has a functional form $\mu = U_c f(U/U_c)$, and the adsorption order parameter (the bound fraction of monomers) $\theta = -\partial\mu/\partial U$ must be a function of a single argument, the reduced potential depth U/U_c.

B. Analytical approach for infinite lattice chains using generating functions

In the case of an infinitely long ideal polymer chain adsorbing onto a surface of a lattice, an analytical description is available in terms of the generating functions (GFs) approach (or the grand-canonical approach). This method was successfully applied for the investigation of helix-coil transitions in polypeptides and polynucleotides and also for the analysis of phase transitions such as adsorption [9,27] as well as mechanical desorption of macromolecules with various stiffness [10] and with excluded volume interactions [13]. The main object in this approach is the GF (or the grand-canonical partition function),

$$\Xi(x) = \sum_{N=1}^{\infty} Z_N x^N, \qquad (7)$$

where Z_N is the partition function of a polymer chain with N units, $x \equiv \exp(\mu)$, where μ is the chemical potential of a monomer unit. Very often it is much easier to calculate the GF rather than a canonical partition function Z_N. Once the GF [Eq. (7)] is known, the partition function Z_N can be formally determined as the coefficients of the expansion of $\Xi(x)$ in powers of x. In the long chain limit, $N \gg 1$, the asymptotic expression for Z_N is even simpler since it is dominated by the *smallest singularity* x_s of $\Xi(x)$: $Z_N \simeq x_s^{-N}$.

The GF approach is particularly efficient in the cases where the chain conformation can be represented as an alternation (not necessary regular) of sequences of different types. This is, of course, also the case for the chain adsorbed onto a substrate because each adsorbed conformation can be represented as a sequence of adsorbed and desorbed groups of monomers. The adsorbed sequences are called trains, and loops separate adsorbed sequences. An end piece of a grafted chain without loops is named a tail. In our ideal chain model different loops and trains do not interact with each other or with the tail.

An expression for the GF of adsorbed chains via GFs of trains, loops, and tails [$\Xi_S(qx,W)$, $\Xi_L(x)$, and $\Xi_T(x)$, respectively] reads [9]

$$\Xi(x) = \frac{[1+\Xi_T(x)]^2\Xi_S(qx,W)}{1-\Xi_S(qx,W)\Xi_L(x)}, \qquad (8)$$

where $q = \exp(U)$ is the statistical weight of an adsorbed monomer unit. The equilibrium chemical potential $\mu(q,W) = \ln x$ is obtained from the smallest of the roots of the following three equations:

$$1 - \Xi_S(qx,W)\Xi_L(x) = 0, \qquad (9)$$

$$\frac{1}{\Xi_S(qx,W)} = 0, \qquad (10)$$

and

$$\frac{1}{1+\Xi_T(x)} = 0, \qquad (11)$$

which are the equations for finding singularities associated with an adsorbed chain with alternating adsorbed and desorbed sequences [Eq. (9)], a completely adsorbed chain, a train, [Eq. (10)], and a desorbed tail [Eq. (11)], which has the same singularity as a desorbed chain in the bulk.

Expressions for $\Xi_S(qx,W)$, $\Xi_L(x)$, and $\Xi_T(x)$ are given below; details of the calculations can be found in the appendix. The GF of trains has the following form:

$$\Xi_S(qx,W) = \frac{\sinh(W\omega)}{\sinh[(W+1)\omega]}, \qquad (12)$$

with

$$\omega = \ln\left[\frac{1-4qx}{2qx} + \sqrt{\left(\frac{1-4qx}{2qx}\right)^2 - 1}\right]. \qquad (13)$$

The GF of loops is

$$\Xi_L(x) = \frac{2x}{1-4x+\sqrt{(1-6x)(1-2x)}} \qquad (14)$$

and the GF of tails is

$$\Xi_T(x) = \frac{2x}{1-6x+\sqrt{(1-6x)(1-2x)}} = \frac{1}{2}\left(\sqrt{\frac{1-2x}{1-6x}}-1\right). \quad (15)$$

These results will be used in the following.

C. Finite lattice chains

For the description of finite ideal chains on the lattice, we used the well-known numerical treatment by transfer-matrix methods. It is based on a Green's function formalism first introduced by Rubin [5,28,29] and later used in the more general theory of Scheutjens and Fleer [2].

To take into account the excluded volume interactions, we used self-avoiding chains on the simple cubic lattice. Numerical simulations were performed using the standard PERM [30,31]. The chain length in our simulations was up to $N = 6400$, and the width of potential was varied in the interval $1 \leqslant W \leqslant 10$. Since this simulation method was recently reviewed in detail [31], we do not describe this method here to save space.

III. RESULTS AND DISCUSSIONS

A. Adsorption-desorption transition point for ideal chains on the lattice and in the continuum

The adsorption-desorption transition point in the GF approach is defined [9] by the condition

$$\Xi_S(q/z_V, W) = 1, \quad (16)$$

where $z_V = 6$ is the number of possible steps on the simple cubic lattice. The critical adsorption energy (see Appendix) is given by

$$U_c(W) = -\ln\left(\frac{2}{3}+\frac{1}{3}\cos\frac{\pi}{2W+1}\right). \quad (17)$$

At $W = 1$ $U_c(1) = \ln(\frac{6}{5})$ in accordance with previous results [5]. At $W \gg 1$, the expansion of Eq. (17) is as follows:

$$U_c(W) \approx \frac{\pi^2}{24}\left(W+\frac{1}{2}\right)^{-2}, \quad (18)$$

which provides an excellent asymptotic approximation of the exact expression [Eq. (17)].

Comparing Eq. (18) with the similar relation for the continuum model as given by Eq. (4), one can notice that the only difference consists of a shift in the value of W by $1/2$ in the lattice model. This shift is quite familiar and appears also when matching the entropy of a continuum chain and a lattice chain in a slit [32]. Interestingly, the same shift was found in describing the scaling properties of an off-lattice chain in a slit [33]. For lattice chains, the width of the adsorption potential cannot be smaller than unity and the maximum critical adsorption energy is equal to $\ln(6/5) = 0.182$. In the model for chains in the continuum the potential width W can be chosen arbitrarily. The critical adsorption energy U_c as a function of the potential width W is presented in Fig. 2 for ideal lattice and continuum chains together with the Monte Carlo data for self-avoiding chains to be discussed shortly.

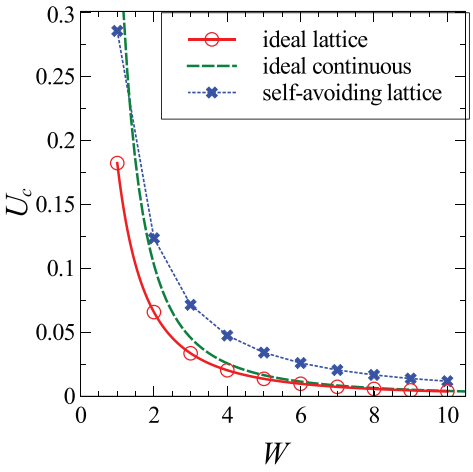

FIG. 2. (Color online) The dependence of the critical adsorption energy U_c on the potential width W for lattice chains without excluded volume interactions [Eq. (17)], continuum chains [Eq. (4)], and self-avoiding lattice chains (according to Table I).

B. Adsorbed fraction θ and sharpness of the adsorption transition $d\theta/dU$ of finite ideal chains

Figure 3 shows the dependence of the average fraction of adsorbed units θ and the slope $\xi = d\theta/dU$ as functions of adsorption parameter U calculated for ideal lattice chains at several chain lengths $N = 100$, 300, 500, and 1000 and ∞ for various potential widths W. The case $W = 1$, Figs. 3(a) and 3(d), was extensively analyzed in the literature before [3] and is presented here only for the sake of comparison. Results obtained by the GF approach for infinitely long chains are shown by solid curves and results calculated numerically by transfer-matrix techniques for finite chains are shown by broken curves.

In all cases for $N \to \infty$ the adsorption occurs as a second-order transition and the curves $\theta(U)$ have a discontinuity in slope ξ at the critical point $U = U_c$. The value of ξ is related to the heat capacity C of the system by the relation $C = \xi U^2$. For wide potentials, the curves $\theta(U)$ shift to the left and become sharper, as can be seen from Figs. 3(b) and 3(c). For $W = 10$ the dependence $\theta(U)$ of infinitely long chain looks like a step function with U_c close to zero. Note that for the wide potential $W = 10$ the behavior of shorter chains $N = 50$–100 looks as if the transition occurs at negative adsorption energy.

C. Universality of adsorption for wide potentials in the case of infinitely long ideal chains

Equation (6) predicts for the continuum model that the adsorbed fraction θ, and, correspondingly, the reduced slope ξU_c for infinite long chains, are functions of a single parameter $U/U_c(W)$. To test this universality for lattice chains we plot the average fraction of adsorbed units θ and the reduced slope ξU_c vs U/U_c for infinitely long ideal lattice chains versus potentials with different widths, $W = 1$, 2, 3, 5, and 10; see Fig. 4. The limiting shape of the curves for $W \gg 1$ is independent of W and coincides with the predictions of the continuum model based on Eqs. (4)–(6). Deviations from the limiting curves are due to lattice effects. Except for the case $W = 1$ they are very small.

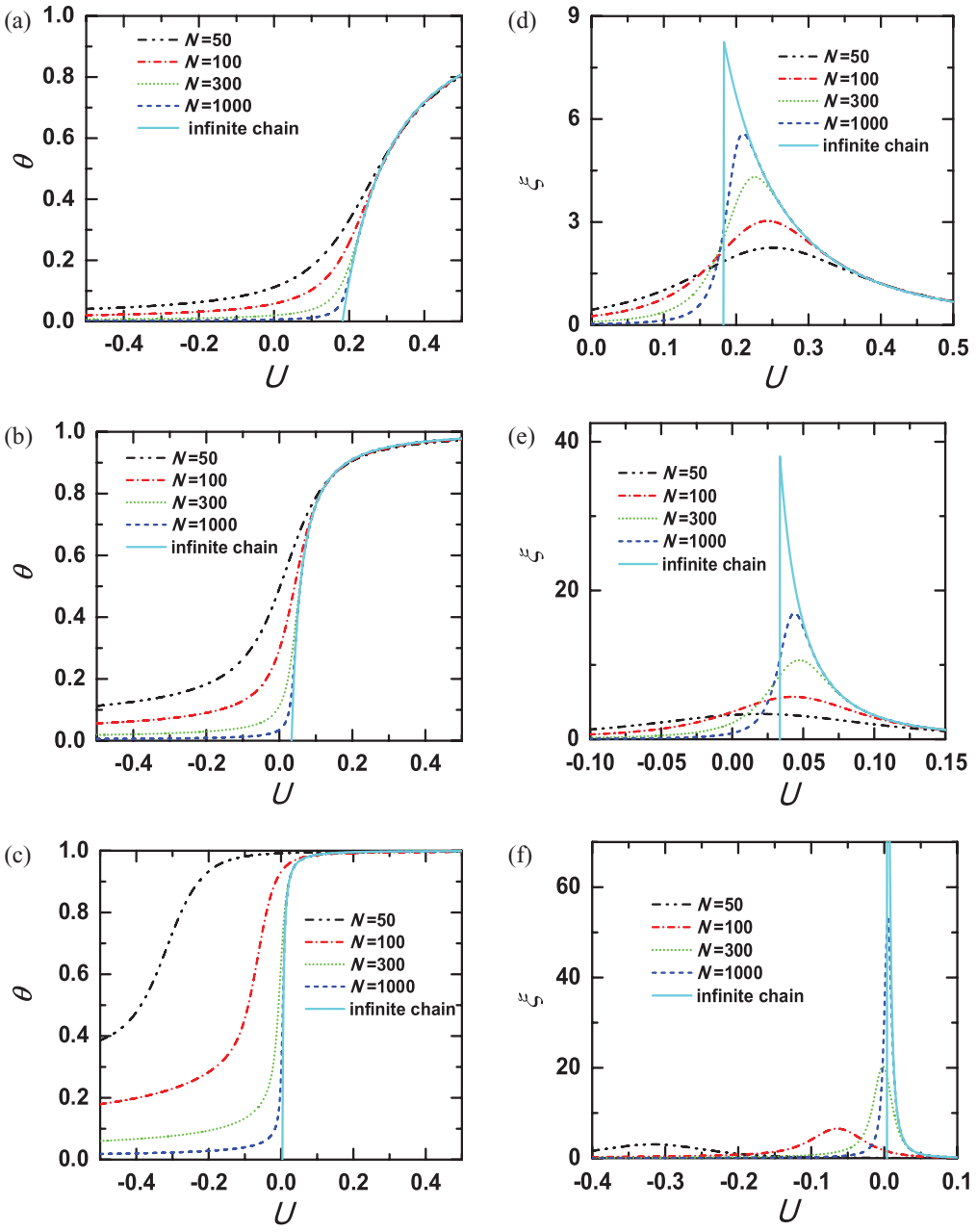

FIG. 3. (Color online) Average fraction of adsorbed units [(a)–(c)] and the transition sharpness $\xi = d\theta/dU$ [(d)–(f)] as functions of adsorption energy U calculated for the potential widths $W = 1$ (a), $W = 3$ (b), and $W = 10$ (c). Several values of chain lengths are chosen, as indicated.

At the transition point, the slope experiences a jump. The maximum reduced slope for $W = 1$ is $(25/3)\ln(6/5) \approx 1.519$, and for the continuum limit $W \to \infty$ is $\pi^2/8 \approx 1.234$.

D. Determination of the transition points for self-avoiding lattice chains

Determination of the adsorption-desorption transition point for chains with excluded volume interactions is always a difficult problem. To estimate the transition point for self-avoiding lattice chains, Krawczyk *et al.* [34] calculated the heat capacity as a function of the adsorption parameter and extrapolated the position of the maximum to infinite chain length N. This method is not very accurate and has an error of a few percentages. Janse Van Rensburg and Rechnitzer [35] demonstrated that the analysis of heat capacity data has many pitfalls.

In the present work we use the method suggested by Grassberger [36], which is based on the scaling properties of the partition function. For a single polymer chain grafted onto an inert solid plane (without any attractive interaction acting on the monomers) the partition function $Q(N)$ scales as

$$Q(N) \sim \mu^N N^{\gamma_1 - 1}. \tag{19}$$

The values of the effective coordination number on a simple cubic lattice $\mu = 4.6840386 \pm 0.0000011$ and the

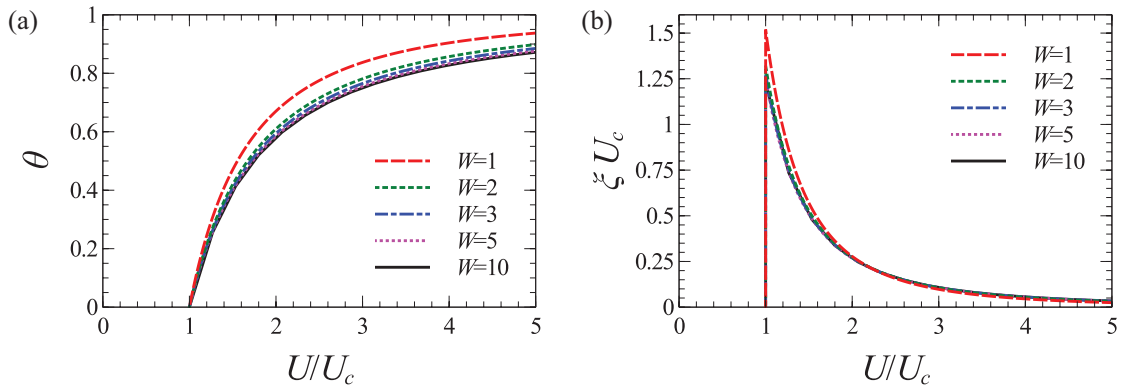

FIG. 4. (Color online) Average fraction of adsorbed units θ (a) and reduced transition sharpness ξU_c (b) plotted versus reduced adsorption energy U/U_c for infinitely long ideal lattice chains. Several values of potential widths W are chosen, as indicated.

critical exponent $\gamma_1 = 0.6786 \pm 0.0012$ are given in Ref. [36]. De Gennes [20,21] and Barber *et al.* [37] demonstrated that the polymer adsorption on the plane in the limit of the infinite chain is closely related to the surface critical phenomena in the m vector model of ferromagnets in a semi-infinite geometry in the limit $m \to 0$. Based on the above analogy Eisenriegler *et al.* [19] described the scaling properties of a long chain near a wall on the basis of the results of the field theory for magnetic systems. It was shown that the adsorption transition in the magnetic analogy corresponds to a multicritical point, where a critical line of $(d-1)$-dimensional surface transitions meets the bulk d-dimensional criticality ("surface-bulk multicritical point"). According to this analogy, at the adsorption transition point U_c the partition function $Q_s(N)$ scales similarly as

$$Q_s(N) \sim \mu^N N^{\gamma_1^s - 1}, \tag{20}$$

with the same value of μ but with a different critical exponent, γ_1^s. Its value was obtained from a second-order ϵ expansion [38], $\gamma_1^s \simeq 1.24$, and from the massive field theory [39], $\gamma_1^s = 1.207$. The numerical estimation for self-avoiding walks (SAWs) at $W = 1$ [36] gives $\gamma_1^s = 1.226 \pm 0.002$. Estimation of this critical exponent (and other universal properties related to the adsorption transition) is a difficult task, because it requires that U_c should be known very precisely. However, as we shall see, the estimation of U_c for SAWs is highly nontrivial and must be done simultaneously with the estimation of the various critical exponents. Adsorption of a flexible self-avoiding chain on a plane with the actual width of the potential, W, will be described by the same exponent γ_1^s as long as it belongs to the universality class of short-ranged potentials (W being much smaller than the gyration radius of the chain).

Grassberger [36] suggests that γ_1^s can be found exactly at the critical point from Eq. (20) in the asymptotic limit of large N as

$$\gamma_{1,\mathrm{eff}}^s(N) = 1 + \ln\left[\frac{Q_s(2N)}{Q_s(N/2)\mu^{3N/2}}\right] \Big/ \ln 4 \approx \gamma_1^s(N), \tag{21}$$

which should be N independent. Corrections to scaling give rise to some weak dependence on N for shorter chains that disappears with the increase in N. Renormalization group theory [4,38–40] implies that these corrections show up by modifying Eq. (20) as

$$Q_s(N) \propto \mu^N N^{\gamma_1^s - 1}(1 + \text{const}\ N^{-\Delta_s} + \cdots), \tag{22}$$

where $\Delta_s (<1)$ is the leading correction to scaling exponent. From Eqs. (21) and (22) it is easy to show that, for $N \to \infty$,

$$\gamma_1^s(N) = \gamma_1^s + cN^{-\Delta_s} \pm \cdots, \tag{23}$$

where c is a (nonuniversal) constant. However, if the adsorption energy is slightly off, the exact critical value the apparent exponent $\gamma_{1,\mathrm{eff}}^s = \gamma_1^s(N,U)$ demonstrates a noticeable variation that becomes even more prominent at large N rather than disappearing. In particular, when the adsorption energy is less than the critical value, the curve of $\gamma_{1,\mathrm{eff}}^s$ drifts downwards towards a much lower value of $\gamma_1^s(N)$. On the other side (stronger adsorption), the apparent $\gamma_{1,\mathrm{eff}}^s$ curves upwards since the scaling form of the partition function acquires an extra exponential factor.

With the PERM, the partition sum can be estimated directly and very accurately. Therefore, this way of data analysis is perfectly suited to the estimation of the critical adsorption point U_c. It is based on the fundamental relation [Eq. (20)]; the value of $\gamma_{1,\mathrm{eff}}^s$ must converge to a constant in the limit of large N and the numerical value of this constant γ_1^s is rather well known and must be the same for all values of the potential width W.

The results of the calculation of $\gamma_{1,\mathrm{eff}}^s$ according to Eq. (21) are shown in Figs. 5(a) and 5(b) for two values of W, $W = 1$ and $W = 5$. As can be seen, the value of $\gamma_{1,\mathrm{eff}}^s$ practically does not depend on N at the critical point U_c. This fact implies that the constant c in Eq. (23) is rather small, but there is no guarantee that a similar fast convergence to the asymptotic limit occurs for other quantities, too.

Another popular method for the estimation of the transition point is based on the behavior of parallel and perpendicular components of the gyration radius. Descas *et al.* [41,42] used scaling arguments showing that, at the transition point, the ratio $R_{g\perp}/R_{g\parallel}$ should be independent of N. This criterion has been applied previously by Metzger *et al.* [16] and later by Bhattacharya *et al.* [15] to determine the critical point for off-lattice model chains with $N < 200$. Having the advantage of a much more precise method based on the direct evaluation of the partition function we can follow the N dependence of the ratio $\langle R_{g\perp}^2 \rangle / \langle R_{g\parallel}^2 \rangle$ and, therefore, evaluate

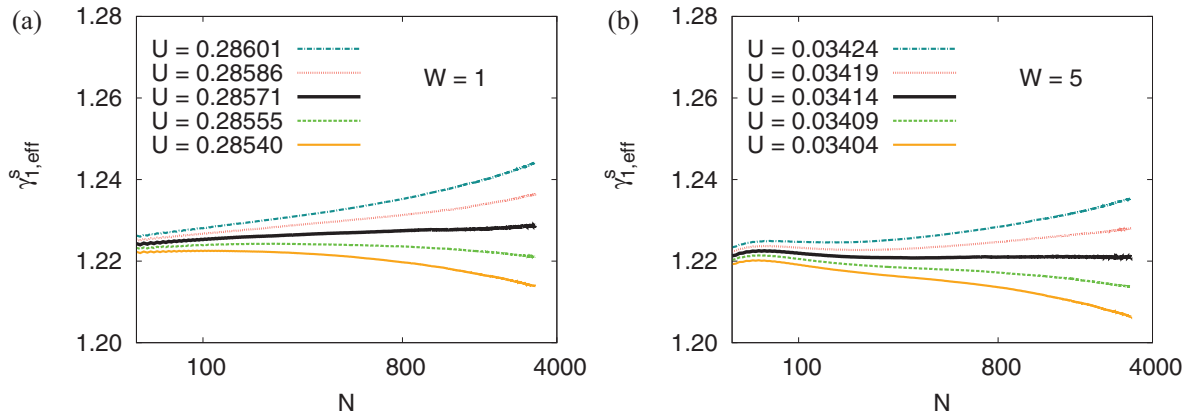

FIG. 5. (Color online) Effective exponents $\gamma^s_{1,\mathrm{eff}}$ plotted versus N for $W = 1$ (a) and $W = 5$ (b); several values of U are chosen as indicated. The bold curves indicate the behavior at the estimated critical point.

the accuracy of this gyration radius component criterion. It is clear from Fig. 6(a) that in the narrow vicinity of the critical point the ratio increases monotonically up to very large values of N and acquires the asymptotic value only for $N \sim 5000$. One can conclude that an attempt to estimate the critical point using the data for relatively small N will lead to a systematic error in U_c. As the width W of potential increases, the situation is no better. Interestingly, Fig. 6(b) demonstrates that for $W = 5$ the ratio $\langle R^2_{g\perp}\rangle/\langle R^2_{g\|}\rangle$ behaves as a decreasing function of N for $N > 100$; the asymptotic value is still reached only for $N \sim 5000$. The ratio $\langle R^2_{g\perp}\rangle/\langle R^2_{g\|}\rangle$ at the critical adsorption point in the $N \to \infty$ limit is a universal number but for finite N it is affected by corrections to scaling, analogously to Eqs. (22) and (23),

$$\left(\left\langle R^2_{g\perp}\right\rangle/\left\langle R^2_{g\|}\right\rangle\right)_{U=U_c} = C_g[1 + C'_g(W)N^{-\Delta_s} + \cdots]. \quad (24)$$

The amplitude factor C'_g clearly is nonuniversal and seems to change its sign close to $W = 2$ [Fig. 6(c)]. Thus, the variation of W clearly is very useful to estimate the universal constant $C_g \approx 0.320 \pm 0.003$ reliably. Obviously, if a simulation

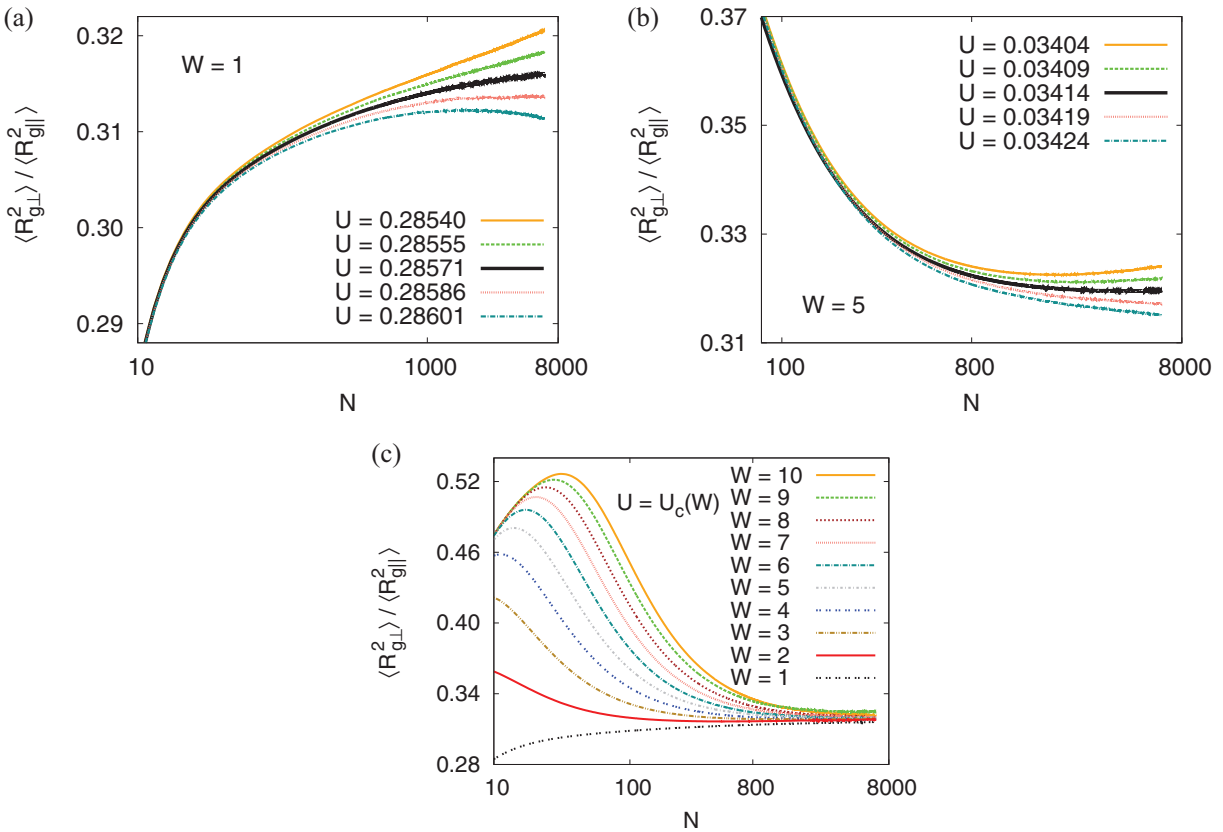

FIG. 6. (Color online) Ratio between the mean-squared gyration radius components perpendicular and parallel to the surface, $\left\langle R^2_{g\perp}\right\rangle/\langle R^2_{g\|}\rangle$, plotted versus N. Data are for $W = 1$ (a) and $W = 5$ (b) and for $1 \leqslant W \leqslant 10$ at $U = U_c$ (c). In (a) and (b) the dependencies at the critical point are shown by bold curves; several values of U are chosen as indicated.

TABLE I. Estimates of the critical energy U_c, the surface critical exponent γ_1^s, the crossover exponent ϕ, and the universal ratio $\langle R_{g\perp}^2\rangle/\langle R_{g\|}^2\rangle$ at $U = U_c$ for a self-avoiding chain interacting with a surface potential of width W on a simple cubic lattice.

W	U_c	γ_s	ϕ	$\langle R_{g\perp}^2\rangle/\langle R_{g\|}^2\rangle$
1	0.2857(1)	1.224(3)	0.483(2)	0.316(2)
2	0.1235(2)	1.223(2)	0.483(2)	0.317(2)
3	0.0714(3)	1.222(2)	0.482(2)	0.318(2)
4	0.0474(2)	1.222(2)	0.482(2)	0.319(3)
5	0.0341(2)	1.221(2)	0.482(3)	0.319(3)
6	0.0259(1)	1.221(4)	0.483(4)	0.320(3)
7	0.0204(3)	1.220(5)	0.481(4)	0.320(3)
8	0.0166(2)	1.220(5)	0.482(4)	0.320(3)
9	0.0138(2)	1.210(20)	0.478(8)	0.325(6)
10	0.0117(2)	1.220(20)	0.480(8)	0.322(6)

method does not allow a direct evaluation of the partition function, the gyration component criterion for localizing the transition may still be quite practical if large-enough chain lengths are available. However, all the subsequent conclusions that crucially depend on the accuracy of U_c have to be taken with great caution.

Table I summarizes the results obtained for self-avoiding walks on the simple cubic lattice with the adsorption potential width W in the range from 1 to 10. These include the value of the critical energy U_c, the surface critical exponent γ_1^s, the ratio between the gyration radius components $\langle R_{g\perp}^2\rangle/\langle R_{g\|}^2\rangle$, and the crossover exponent ϕ to be discussed later. Note that the estimated critical exponents do not depend on W as expected within the same universality class.

We note that a similar idea, variation of a parameter of the potential to check for the magnitude of corrections to scaling (and possibly find a case where the amplitude of the leading correction to scaling changes its sign, allowing a more accurate estimation of universal properties), has been successfully used in other contexts, e.g., Monte Carlo simulations of critical phenomena in the Ising model. There one can use, for instance, a model with both nearest ($J_{\rm nn}$) and next-nearest ($J_{\rm nnn}$) neighbor exchange interactions, their ratio being a parameter to be varied. This concept is easily understood in a real-space renormalization group context, where the criticality is described by a hypersurface in the space of coupling constants, and the renormalization group flow on the critical hypersurface leads to a "fixed point Hamiltonian" $\{J_{\rm nn}^*, J_{\rm nnn}^*, \ldots$; recall that all coupling constants are taken in units of k_BT throughout$\}$. If for a system the couplings are at the critical hypersurface but not on the fixed point, one has nonzero "irrelevant operators", which are renormalized to zero under renormalization group flow but give rise to corrections to scaling [40].

It is also interesting to try this approach to estimate the crossover exponent ϕ, which can be extracted from the adsorption energy $E_s = \sum_{i=1}^{N}\langle\zeta_i\rangle U$, where $\zeta_i = 1$ if the monomer labeled by i has a z coordinate normal to the surface $z_i \leqslant W$ while $\zeta_i = 0$ if $z_i > W$. For large N at $U = U_c(W)$ we must have $E_s \propto N^{\phi}$. The scaling theory [4,19] implies that ϕ is an independent exponent that cannot be related to any standard critical exponents of the self-avoiding walk problem,

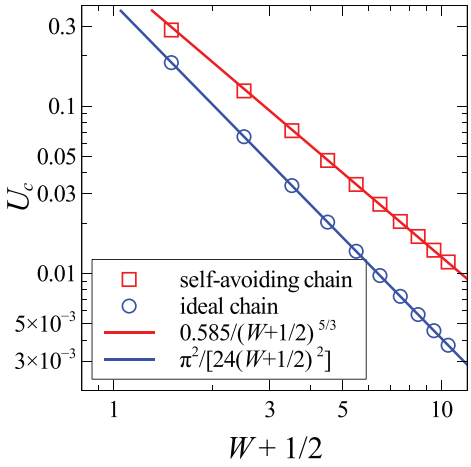

FIG. 7. (Color online) The double logarithmic dependence of the critical adsorption energy for ideal and self-avoiding lattice chains on the potential width $(W + 1/2)$. The two straight lines indicate the power laws, Eqs. (18) and (25).

contrary to early suggestions [20,21]. While early numerical estimates [19] yielded $\phi \approx 0.59$, later numerical studies as well as renormalization group estimates yielded numbers close to the mean-field value ($\phi_{\rm MF} = 1/2$) [35,43]. While Metzger *et al.* [16,17] already noted that for chain lengths $N \leqslant 500$ the simulation results did not yield a clear result, due to the strong correlation between the best estimate for ϕ and the estimated location of the adsorption transition, Descas *et al.* [41,42] again suggested ϕ to be close to the original estimate of Eisenriegler *et al.* [19]. However, the recent work of Grassberger [36] yielded again a much smaller values $\phi = 0.483(2)$. We shall return to this controversy in a later section.

The dependence of the critical adsorption energy U_c on the potential width W for self-avoiding lattice chains was presented before in Fig. 2. A log-log plot suggested by the analytical expression for ideal lattice chains, Eq. (18), reveals a simple scaling form of $U_c(W)$; see Fig. 7. All the Monte Carlo data points are very accurately described by

$$U_c = \frac{0.585}{(W+1/2)^{5/3}}. \tag{25}$$

The physical interpretation for the power law, Eq. (25), will be discussed in the next section.

E. Renormalization and the blob picture at the adsorption critical point

According to the basic tenets of the critical phenomena theory and the polymer-magnetic analogy [19] in the presence of an attractive surface, the chain conformation at critical conditions is self-similar in the $N \to \infty$ limit. One can group the segments of the chain into a blob to match the length scale imposed by the width of the potential, W. For a self-avoiding chain (where in the bulk the radius R scales with the number of segments N as $R \sim N^{3/5}$ or $N \sim R^{5/3}$ [20]), one expects the number of the original segments (g) in the blob to scale as $g \sim W^{5/3}$. Here for simplicity, we take for the exponent ν the Flory values $\nu = 3/5$ rather than the more accurate number $\nu \approx 0.588$ suggested by renormalization

group methods [44,45]. The total energy of the blob in contact with the surface can be estimated as $g(W)U$. From very basic considerations, at the critical condition this energy is of order k_BT or, in reduced units, of order 1. A more concrete statement follows from self-similarity of the critical chain conformation with respect to a direct-space renormalization [40]. Repeated renormalization brings the system to a fixed point which implies that

$$g(W)U_c(W) \to \text{const}, \tag{26}$$

at least for large-enough values of W. The fact that the MC data are very well described by Eq. (25) allows a simple and direct realization of the self-similarity idea. We define the blob size according to $g(W) = B(W + \frac{1}{2})^{5/3}$ and impose a natural condition $g(1) = 1$. This fixes the proportionality coefficient B to give

$$g(W) = \left(\frac{2W+1}{3}\right)^{5/3}. \tag{27}$$

Extending the condition, Eq. (26), down to the lowest value $W = 1$ (which is, to some extent, a brute-force exercise) leads to the following blob picture prediction for the critical adsorption point:

$$U_c(W) = U_c(1)\left(\frac{2W+1}{3}\right)^{-5/3} \tag{28}$$

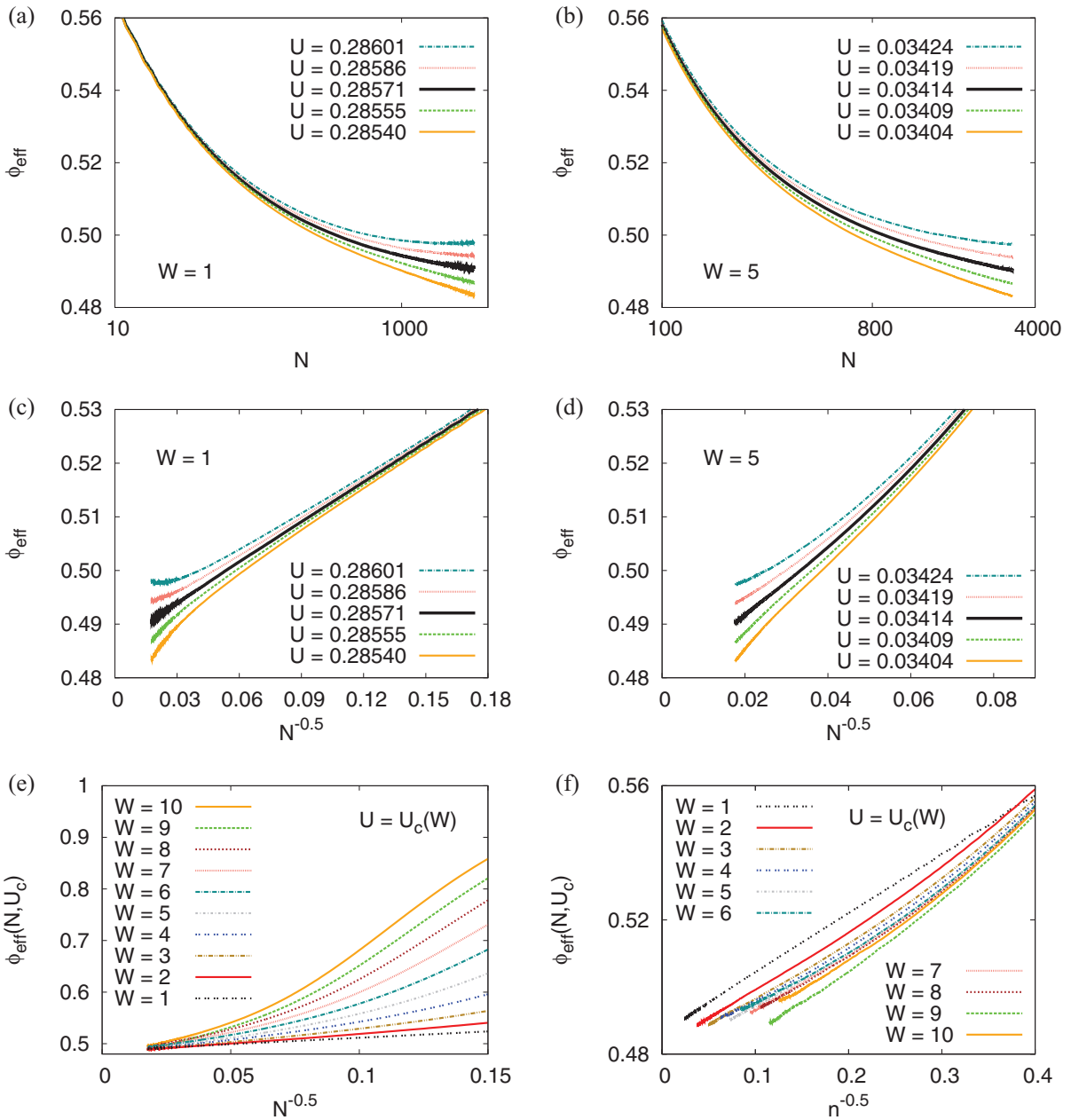

FIG. 8. (Color online) Effective crossover exponent ϕ_{eff} plotted versus N, and $N^{-0.5}$ for $W = 1$ [(a) and (c)] and $W = 5$ [(b) and (d)], respectively. Several values of U are chosen, as indicated. At the critical point U_c, the effective crossover exponent ϕ_{eff} plotted versus $N^{-0.5}$ (e) and $n^{-0.5}$ (f) for $1 \leqslant W \leqslant 10$.

with no fitting parameters. Taking the well-known literature value [36] $U_c(1) = 0.2857$, one arrives at $U_c(W) = 0.562(W + 1/2)^{-5/3}$ Amazingly, this expression describes the Monte Carlo data of Table I quite accurately with the relative error of less than 4% for all W from 2 to 10.

F. Crossover exponent ϕ for SAWs

The crossover exponent ϕ plays a key role in the analysis of polymer adsorption. It determines how the number of contacts scales with N exactly at the critical point [4,19]. It also controls the temperature dependence of the adsorption energy as well as the shape of the density profile in the adsorption region [4,19]. As a surface critical exponent it cannot be deduced from the known bulk critical exponents. Determination of its value has been a subject of extensive work as mentioned above, and the results generated some debate. In particular, it was realized that simulation-based estimates are very sensitive to the accuracy of the critical point estimation. As we are able to determine the critical point with an error at least an order of magnitude smaller than most of the other methods, it is worthwhile to revisit the problem here.

A more refined way of determining ϕ was suggested by Grassberger [36] based on the scaling form for the adsorbed fraction $\theta(N,U,W)$, $\theta(N,U,W) \propto N^{\phi-1}$ as $N \to \infty$. Following the logic explained in Sec. III D, one defines the effective crossover exponent

$$\phi_{\rm eff}(N,U,W) = \ln\left(\frac{4\theta(2N,U,W)}{\theta(N/2,U,W)}\right) \Big/ \ln 4 \qquad (29)$$

and plots it as a function of N in order to catch its asymptotic value. Contrary to the effective exponent $\gamma^s_{1,\rm eff}$, which reaches the asymptotic plateau ($\phi_{\rm eff} \approx \phi$) starting from relatively small N, the apparent crossover exponent contains significant corrections to scaling so eventual extrapolation is required.

The curves of $\phi_{\rm eff}(N,U,W)$ versus $\ln N$ are presented in Figs. 8(a) and 8(b) for two values of W. The central curve always shows the behavior of $\phi_{\rm eff}(N,U,W)$ at the critical point $U_c(W)$ estimated earlier and presented in Table I. Apart from U_c we show other curves for two values U above U_c and two below U_c. For both cases, $W = 1$ and $W = 5$, the effective crossover exponent continues to decrease, even for $N > 5000$. To extrapolate we plot $\phi_{\rm eff}(N,U,W)$ vs $1/\sqrt{N}$, see Fig. 8(c), assuming that corrections to scaling are of order $N^{-1/2}$. A reasonably good linear behavior of the apparent exponent at the best estimate of the critical point supports this assumption. However, for $W = 5$ this plot of $\phi_{\rm eff}$ vs. $1/\sqrt{N}$ exhibits more curvature [Fig. 8(d)], and this reflects a systematic dependence on W [Fig. 8(e)]. However, a much more regular behavior is found when one uses the number of blobs n rather than the number of bonds N as a variable [Fig. 8(f)]. Extrapolated results are summarized in Table I. All the values obtained for different potential width are very close to each other, which is, again, consistent with the fact that we are in a single universality class. It is clear that the value of ϕ is definitely below 0.5 but the difference is quite small.

G. Adsorbed fraction and renormalized segment in finite chains

For finite chains the average fraction of adsorbed units θ generally depends on three parameters: the chain length N and the potential parameters W and U. We have demonstrated that in the limit $N \to \infty$ the potential parameters enter only through the combination $U/U_c(W)$. The blob picture of the chain at the critical adsorption point suggests that finite-size effects should be determined by the number of renormalized segments $n(W) = N/g(W)$, each representing a blob of linear size W. Thus, the adsorbed fraction must have the functional form $\theta(n(W),U/U_c(W))$ with only two independent variables.

In analogy to Sec. III E, we define an ideal W blob containing $g_{id} = ((2W+1)/3)^2$ monomer units. The adsorbed fraction $\theta(n,U/U_c)$ vs U/U_c for ideal lattice chains is presented in Fig. 9 for different potential widths W and different chain lengths N adjusted in such a way that the number of W blobs was fixed as $n = 10$. The nearly universal curve that is obtained in this way demonstrates the correctness of such scaling.

The same scaling ansatz was checked for self-avoiding polymer chains with the appropriate changes in the expressions for $g(W)$ and $U_c(W)$ defined now according to Eqs. (25) and (27), respectively. Figure 10 displays the adsorbed fraction vs U/U_c for three different values of the number of $(W + 1/2)$ blobs, $n = 10$, 20, 80, where each curve includes data points

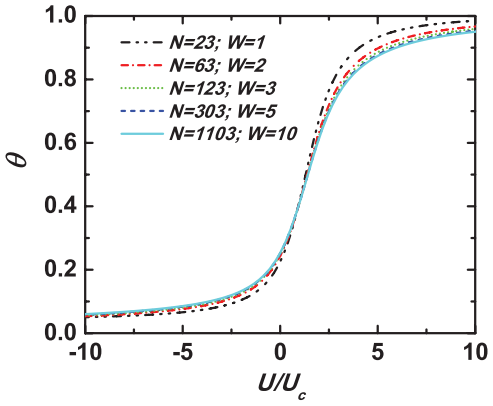

FIG. 9. (Color online) Average fraction of adsorbed units, θ, for ideal lattice chains as a function of reduced adsorption energy, U/U_c, calculated for different chain lengths, N, and several potential widths, W, keeping the same amount of $(W + 1/2)$ blobs as $n = 10$.

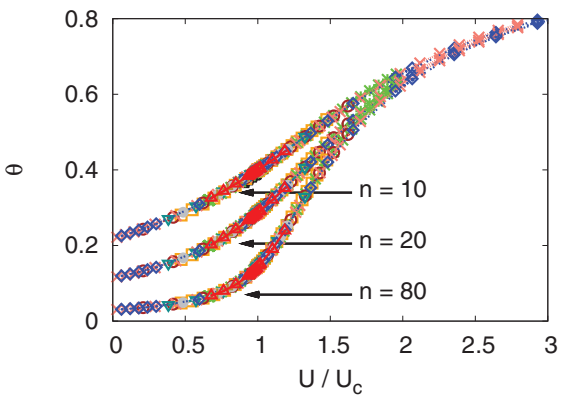

FIG. 10. (Color online) Average fraction of adsorbed units, θ, plotted versus U/U_c for chains with excluded volume interactions. Chain lengths are chosen such that the numbers of $(W + 1/2)$ blobs are fixed at $n = 10$, 20, and 80 (from top to bottom) for $1 \leqslant W \leqslant 10$.

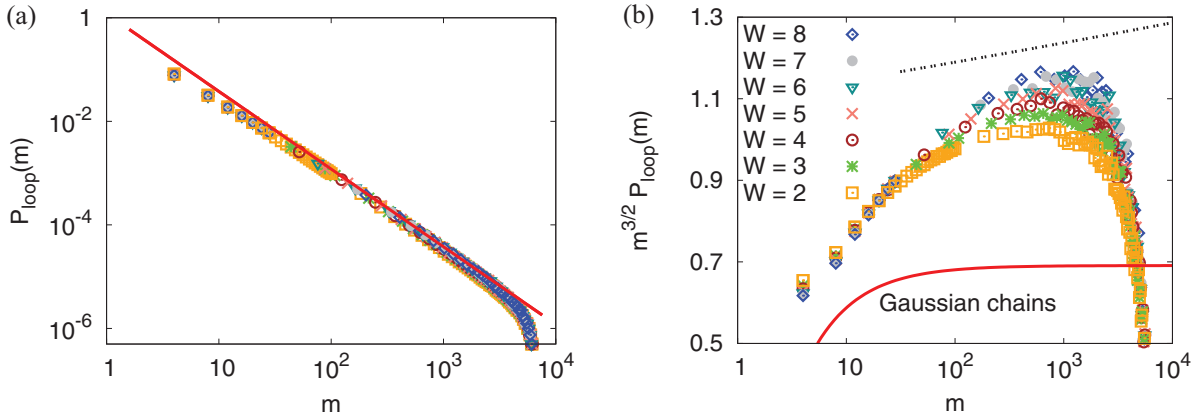

FIG. 11. (Color online) (a) Loop length distribution $P_{\text{loop}}(m)$ of SAWs with chain length $N = 6400$ at the adsorption transition point $U_c(W)$ for $1 \leqslant W \leqslant 8$. (b) $m^{3/2} P_{\text{loop}}(m)$ plotted versus m. The solid curves indicate the asymptotic behavior for ideal lattice chains according to the leading term and the next terms of Eq. (30) in [(a) and (b)], respectively. For a self-avoiding chain at the critical point the theory predicts almost the same slope $(-1-\phi)$ for $\phi \approx 0.483$ in (a). Note that the downward bending trend of the slope for $N \geqslant 2000$ is an effect due to the finiteness of chain length of our SAWs. The dashed straight line in (b) shows the slope predicted for the asymptotic power law for SAWs.

for $1 \leqslant W \leqslant 10$. Collapse of the data strongly supports the scaling ansatz.

At this point we stress that the $(W + 1/2)$ blobs introduced to match the potential range have the meaning of renormalized segments that can belong to the adsorbed trains as well as to loops or to the tail. They should not be confused with the common notion of adsorption blobs defined to match the adsorption correlation length. In contrast to the $(W + 1/2)$ blob, which depends only on the width of the potential but not on its depth nor on the chain length, the size of the adsorption blob may change dramatically, depending on the proximity to the critical point.

H. Loop and tail distributions at the transition point

The loop length distribution for the ideal lattice infinite chain at the critical point can be derived from the corresponding GF $\Xi_L(x)$, Eq. (14), by performing its singularity analysis (see, e.g., Ref. [46]): The probability to find loops containing m segments is

$$P_{\text{loop}}(m) \approx m^{-3/2} \sqrt{\frac{3}{2\pi}} \left(1 - \frac{3}{2m} + \cdots\right). \tag{30}$$

For a self-avoiding chain at the critical point the distribution of loop lengths has a form $P_c(m) \sim m^{-1-\phi}$ [13]. The crossover exponent ϕ determines the behavior of the chemical potential near the critical point $\mu_{\text{ads}} \sim (U - U_c)^{1/\phi}$ and characterizes the order of the phase transition. Our best estimates of the crossover exponent $\phi \approx 0.483$ for $1 \leqslant W \leqslant 10$ are presented in Table I. MC results of the loop length distribution $P_{\text{loop}}(m)$ for SAWs with $N = 6400$ at the critical point under the potential of various widths $1 \leqslant W \leqslant 8$ are shown in Fig. 11. The loop distribution is independent of the potential width (which is to be expected according to the loop definition) and is very well described by a power law with the power $-(1 + \phi)$ predicted by the theory. Since ϕ is very close to $1/2$, the leading power law of the loop distributions at the transition points for ideal and self-avoiding chains almost coincide [Fig. 11(a)].

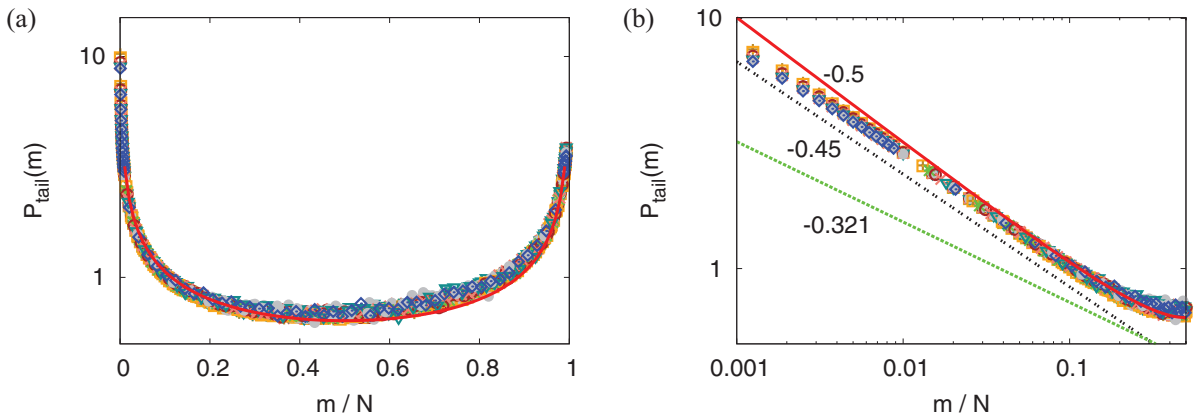

FIG. 12. (Color online) (a) Tail length distribution of SAWs with $N = 6400$ at the critical point $U_c(W)$ for $1 \leqslant W \leqslant 8$. The solid curve shows the distribution of continuum Gaussian chains, Eq. (32). (b) Same data as shown in (a) but plotted on a log-log scale for $m/N < 0.5$. The best fit line with slope -0.45, the line with predicted slope $-(1 - \gamma_1) = -0.321$ in Ref. [13], and the line with slope $-1/2$ predicted for ideal chains are also shown for comparison.

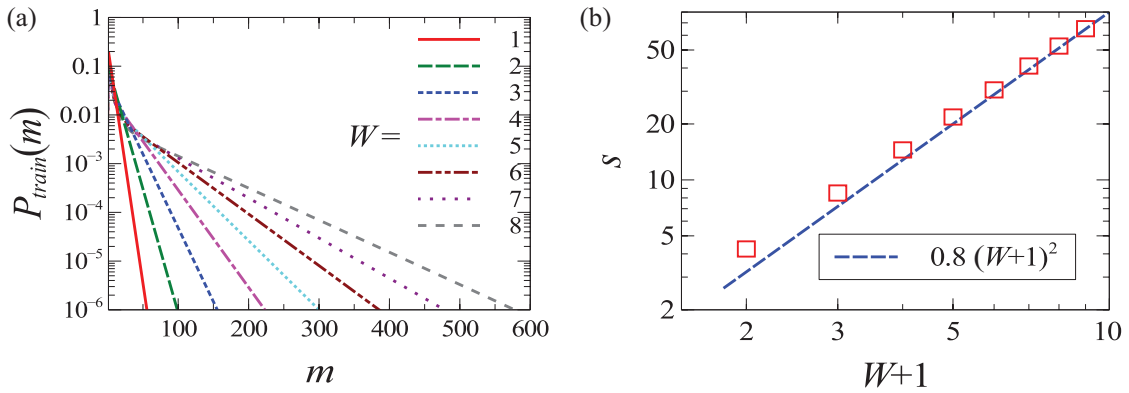

FIG. 13. (Color online) (a) Train length distribution of ideal lattice chains with $N = 1000$ at the critical points $U_c(W)$ for $1 \leqslant W \leqslant 8$. Several values of W are included, as indicated. (b) Typical train length S extracted from the exponential part of the distribution $P_{\text{train}}(m)$ in (a) plotted versus $(W + 1)$ on a log-log scale.

Figure 11(b) shows corrections to $m^{-3/2}$ scaling for ideal and self-avoiding chains. Ideal chains are described by Eq. (30). In the case of SAWs, corrections stem from three different origins. First, for small loops, the probability is noticeably reduced, similar to what is seen in ideal chains. Second, there is a consistent (though small) correction due to the difference between the ideal and the excluded volume loop exponents ($3/2$ vs $1 + \phi$). This factor, i.e., $m^{-1-\phi}$, is shown in Fig. 11(b) by the dashed line. Finally, a sharp downward turn in the MC data at larger values of m is due to finite chain length, which results in a cut-off of the distribution tail.

The tail length distribution of ideal lattice infinite chains can be derived from the GF $\Xi_T(x)$. At the adsorption transition point it has the form

$$P_{\text{tail}}(m) \approx \frac{1}{\sqrt{6\pi m}}\left(1 + \frac{1}{16m^2} + \cdots\right). \tag{31}$$

The distribution of infinite-length self-avoiding chains at the critical point was proposed in [13] as $P_{\text{tail}}(m) \sim m^{-\beta}$, where $\beta = 1 - \gamma_1 \approx 0.3214$.

The tail length distribution of continuum Gaussian chains was calculated in Ref. [24]. In contrast to the GF approach, the continuum theory can operate with the partition function of a finite polymer chain. According to the continuum theory, the tail length distribution at the critical point is nonmonotonic and symmetric:

$$P_{\text{tail}}(m) \approx \frac{N}{\pi\sqrt{m(N-m)}}. \tag{32}$$

Analytical predictions for infinite chains mentioned above, by the very nature of the grand-canonical ensemble approach, can describe only the falling branch of the tail length distribution corresponding to $m \ll N$. Monte Carlo data for the tail length distribution of SAWs with $N = 6400$ at the critical point are presented in Fig. 12 for the potential widths $1 \leqslant W \leqslant 8$. The analytical equation for the ideal chain, Eq. (32), is shown by a solid curve. The tail length distribution obtained in our simulations is nonmonotonic but has some asymmetry, in contrast to Eq. (32). The fact that the distribution is completely insensitive to the potential width is quite natural in view of the universality class argument. The log-log plot of the tail length distribution at relatively small values of $m < N/2$ is compared to infinite chain predictions in Fig. 12(b). The best-fit slope -0.45 is closer to the predicted value for ideal chains rather than to the scaling prediction of Ref. [13].

I. Train length distribution at the transition point

It is well known that the train length distribution of ideal lattice chains decays exponentially [$P_{\text{train}} \propto \exp(-m/S)$] for $W = 1$ at the critical point [47] and is given by

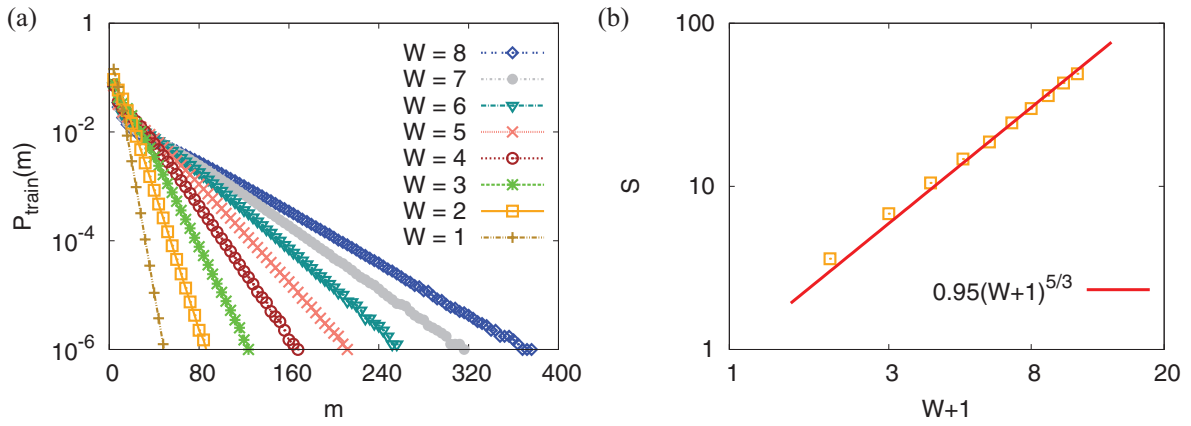

FIG. 14. (Color online) Same as Fig. 13 but data are for SAWs with $N = 6400$.

$\ln P_{\rm train}(m) = m\ \ln(4/5) + \text{const}$. For $W > 1$ the train length distributions do not show exactly an exponential decay. Numerical transfer-matrix calculations for finite ideal chains of length $N = 1000$ are presented in Fig. 13(a). The decay length of the exponential part of the distribution, S, has the meaning of a typical train length; its variation with W is shown in Fig. 13(b). The ideal-chain scaling, $S \propto (W+1)^2$, is reasonably well satisfied. The shift of the potential width by 1 is consistent with the lattice effect mentioned above in the discussion of the scaling form of critical energy and the blob size. The only difference is that the definition of a train includes boundary conditions at two surfaces instead of one, hence, the doubling of the 1/2 shift.

Similar curves for self-avoiding chains are presented in Fig. 14. The only noticeable difference is that the typical train length now scales as $S \propto (W+1)^{5/3}$.

IV. DISCUSSION

Two aspects are worth discussing in connection to the results presented above. The first relates to the debate concerning the value of the crossover exponent ϕ. Descas *et al.* [42] clearly demonstrated that there exists a strong correlation between the best estimates for the critical adsorption point and for the crossover exponent. However, the situation is even more complicated. The PERM method allows a very accurate determination of the critical point: The error is less than 0.05% in the case $W = 1$, which is at least an order of magnitude better than when using common MC methods that do not allow direct evaluation of the partition function. The effective crossover exponent $\phi_{\rm eff}(N)$ was evaluated as the slope of the $\ln m_s$ vs $\ln N$ curve, where m_s is the number of contacts with the surface. The slope is taken over the interval from $N/2$ to $2N$, the two points being symmetric on the log scale, thus providing a central derivative evaluated at point $\ln N$. The results of Fig. 8(a) shows that the slope keeps decreasing up to the largest values of N explored in our simulation. This suggests important corrections to scaling due to subleading terms that can be summarized as $\phi_{\rm eff}(N) \approx \phi(1 + AN^{-\Delta_s})$, where Δ_s is close to 0.5. Note, that since ϕ by itself is close to 0.5, the subleading term with exponent t in the asymptotic expansion of the number of contacts $m_s \sim N^{\phi} + BN^{t}$ is a very weak function of N, possibly even a constant or a logarithm. From the practical point of view, any simulation in a limited range of N (e.g., $50 < N < 200$) will inevitably produce the data that can be described only by an effective crossover exponent, even if the critical point is localized exactly.

Second, we think that our results may help to rationalize simulation results on polymer adsorption found in the literature for various polymer models. Bhattacharya *et al.* [13] used an off-lattice model with a rectangular surface potential; the critical energy was estimated to be $U_c \approx 1.69$. On the other hand, a much-studied standard simple cubic lattice model has the critical energy of 0.286. The question of why these values differ by about an order of magnitude is never addressed since the common wisdom states that the critical energy is model dependent and one should concentrate on the universal features of the phenomenon. This is, of course, true, but an explanation of these huge variations would be satisfying. Inspection of the model [13] shows that the potential was chosen to be very narrow, $W \approx 0.4b$, where b is the segment length. For this potential Eq. (4) gives $U_c \approx 2.5$. Keeping in mind that the continuum description may not be good for $W < b$ and does not account for the excluded volume effects, the difference between the two values is rather modest.

Note that if the potential width is large compared to the Kuhn segment, both lattice and off-lattice ideal chain models can be naturally further reduced to a continuum description in terms of Brownian trajectories. Critical point determination and weak adsorption can be reduced to an eigenvalue problem of the Edwards equation. Standard dimensional analysis of the eigenvalue problem leads to a very general result: an affine stretching of the potential curve by a factor of W always changes the critical energy parameter by a factor of W^{-2} irrespective of the specific shape of the potential; this is a generalization of the effect discussed above for lattice chains. MC simulation results and their analysis presented above suggest that a similar scaling of the critical energy by factor $W^{-5/3}$ should be valid for the critical point in the case of chains with excluded volume interactions.

With off-lattice models the choice of the potential shape allows for more variation and this results in a very broad range of the critical energy values. For example, two adsorption potentials were used by Metzger *et al.* in off-lattice MC simulations [16]:

$$U_1(z) = \epsilon(z^{-9} - f_1 z^{-3}), \tag{33}$$

$$U_2(z) = \epsilon(z^{-10} - f_2 z^{-4}), \tag{34}$$

with $f_1 = 100$ and $f_2 = 2.5$. The obtained critical value of the adsorption energy was $\epsilon_c \approx 0.01$ in the first case and $\epsilon_c \approx 1.6$ in the second case. These potentials could be characterized by their depth $U_{\rm min}$ and position of the minimum $z_{\rm min}$. One readily finds that $U_{1\rm min} = -2\epsilon(f_1/3)^{3/2}$ and $z_{1\rm min} = (3/f_1)^{1/6}$ while $U_{2\rm min} = -(3/2)\epsilon(2f_2/5)^{5/3}$ and $z_{2\rm min} = (5/2f_2)^{1/6}$. So when we consider the product $U_{\rm min}z_{\rm min}$ at $\epsilon = \epsilon_c$ we find a number $-0.02(f_1/3)^{4/3} \approx -2.15$ with respect to Eq. (33), but $-2.4(2f_2/5)^{3/2} \approx -2.4$ in the second case. Compared in this way, the energy scales for adsorption are not so dissimilar as on first sight. However, such a scaling differs from the scaling appropriate for the square-well potential.

ACKNOWLEDGMENTS

We are grateful to the Deutsche Forschungsgemeinschaft (DFG) for financial support: L.I.K., A.A.P., and A.M.S. received support under Grants No. 436 RUS 113/863/0-2 and No. SCHM 985/13-1, while H.-P.H. was supported under Grant No. SFB 625/A3. We are also grateful to the John von Neumann Institute for Computing (NIC Jülich) for a generous grant of computer time.

APPENDIX: CALCULATION OF GENERATING FUNCTIONS

The GF for trains, loops, and tails is expressed as

$$\Xi_i(x) = \sum_{n=1}^{\infty} \Omega_i(n)\, x^n, \tag{A1}$$

where $i = \{S, L, T\}$, where $\Omega_i(n)$ is the number of conformations corresponding to each sequence of the type i of length n.

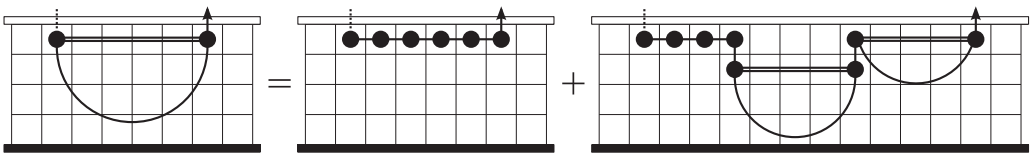

FIG. 15. Decomposition of a loop in a slit. Black boundary is solid (impenetrable) while white boundary is penetrable.

1. Calculation of the generating function of adsorbed sequences and loops

In contrast to the "traditional" lattice model of polymer adsorption where the monomer-surface interaction takes place only in the first lattice layer adjacent to the adsorbing plane, in the case of a square-well potential of finite width W, a train can be considered as being "squeezed" into a slit of the width W. Moreover, each train connects two loops (or the last loop and the tail). Hence, each train itself can be considered as a *loop* localized in the slit of a width W: It starts and ends in the layer $z = W$ and has monomer units at $z < W$. The last monomer, however, is followed by the step to the layer $z = W + 1$. Obviously, the GF depends on the width W; therefore, we denote this partition function as $\Xi_S(x,W)$. The GF of "true" loops in the half-space is obtained by taking the limit $W \to \infty$, hence, $\Xi_L(x) = \Xi_S(x,\infty)$.

To calculate the GF of such "localized loops" we should take into account the following two possibilities schematically shown in Fig. 15:

(1) The loop can never enter the interfacial layer $z = W + 1$.

(2) The loop starts with several steps in the interfacial layer $z = W$ and then enters the next-to-interfacial layer, $z = W - 1$, and forms a loop starting and ending in this layer and returns to the interfacial layer where a new loop is formed.

In terms of the GFs the decomposition presented in Fig. 15 is written as follows:

$$\Xi_S(x,W) = \frac{x}{1-z_S x}\cdot\frac{z_V - z_S}{2} + \frac{x}{1-z_S x}\cdot\frac{z_V - z_S}{2}\Xi_S(x,W-1)\Xi_S(x,W), \tag{A2}$$

where z_V and z_S are the number of possible lattice steps that can be made in three and two dimensions (i.e., in the bulk and in the surface), respectively. For the simple cubic lattice, $z_V = 6$ and $z_S = 4$.

Therefore, we obtain the following recursion relation for $\Xi_S(x)$:

$$\Xi_S(x,W) = \frac{z_V - z_S}{2}x\left[1 - z_S x - \frac{z_V - z_S}{2}x\,\Xi_S(x,W-1)\right]^{-1}. \tag{A3}$$

The starting point (the initial condition) is the GF in the zero width ($W = 0$) slit: $\Xi_S(x,0) = 0$. Applying Eq. (A3) we obtain

$$\Xi_S(x,1) = \frac{x(z_V - z_S)/2}{1 - z_S x}, \tag{A4}$$

where one easily recognizes the GF of the chain on the surface. By iterating Eq. (A3) one can see that $\Xi_S(x)$ can be represented in the form of generalized continued fraction,

$$\Xi_S(x,W) = \cfrac{x(z_V - z_S)/2}{1 - z_S x - \cfrac{x^2(z_V - z_S)^2/4}{1 - z_S x - \cfrac{x^2(z_V - z_S)^2/4}{1 - \dots}}}. \tag{A5}$$

It is known that a continued fraction is a rational function that can be represented as a ratio of two polynomials [48]:

$$\Xi_S(x,W) = \frac{A_W(x)}{B_W(x)}, \tag{A6}$$

where the polynomials $A_n(x)$, $B_n(x)$ satisfy the same second-order recurrence relation (with different initial conditions), namely

$$T_{n+2}(x) = (1 - z_V x)T_{n+1}(x) - x^2\left(\frac{z_V - z_S}{2}\right)^2 T_n(x), \tag{A7}$$

where $T = \{A,B\}$. The initial conditions are

$$A_0(x) = 0, \quad A_1(x) = x\frac{z_V - z_S}{2}, \tag{A8}$$

$$B_0(x) = 1, \quad B_1(x) = 1 - z_S x. \tag{A9}$$

Using these initial conditions, the solution of Eq. (A7) for $A_n(x)$ and $B_n(x)$ can be found,

$$A_n(x) = \frac{z_V - z_S}{2\Delta}x\left[\left(\frac{1 - z_S x + \Delta}{2}\right)^n - \left(\frac{1 - z_S x - \Delta}{2}\right)^n\right], \tag{A10}$$

$$B_n(x) = \frac{1}{\Delta}\left[\left(\frac{1 - z_S x + \Delta}{2}\right)^{n+1} - \left(\frac{1 - z_S x - \Delta}{2}\right)^{n+1}\right], \tag{A11}$$

where $\Delta = \sqrt{(1 - z_V x)[1 - (2z_S - z_V)x]}$. Then

$$\Xi_S(x,W) = (z_V - z_S)x\frac{(1 - z_S x + \Delta)^W - (1 - z_S x - \Delta)^W}{(1 - z_S x + \Delta)^{W+1} - (1 - z_S x - \Delta)^{W+1}}. \tag{A12}$$

This expression can be expressed in more compact form,

$$\Xi_S(x,W) = \frac{\sinh(W\varphi)}{\sinh[(W+1)\varphi]}, \tag{A13}$$

where

$$\cosh\varphi = \frac{1 - z_S x}{(z_V - z_S)x}, \tag{A14}$$

or, equivalently,

$$\varphi = \ln\left[\frac{1 - z_S x}{(z_V - z_S)x} + \sqrt{\frac{(1 - z_S x)^2}{(z_V - z_S)^2 x^2} - 1}\right]. \tag{A15}$$

This result completely coincides with the generating function of a loop in the slit obtained by DiMarzio and Rubin 30 years ago using the transfer matrix approach (with the only difference being an additional factor $(z_V - z_S)/2$, which is the weight of the step preceding the first monomer unit of the loop).

From Eq. (14) the GF of the loops in thee half-space $\Xi_\infty(x)$ is readily obtained:

$$\Xi_L(x) = \Xi_S(x,\infty) = \frac{(z_V - z_S)x}{1 - z_S x + \Delta}. \tag{A16}$$

Now let us analyze the obtained expression.

2. Adsorption-desorption transition point

In the adsorption-desorption transition point the smallest singularity corresponding to the adsorbed chain state is equal to $x_V = 1/z_V$. As was shown by Birshtein [9], the transition point $\Xi_L(1/z_V) = 1$ and the equation for finding the critical adsorption energy (critical depth of the adsorption potential U) has a very simple form,

$$\Xi_S(q/z_V, W) = 1, \tag{A17}$$

where $q = e^U$ is the statistical weight of the adsorbed segment (by "adsorbed" we mean a segment that "falls into the potential range", i.e., is localized in the attraction zone $0 < x < W$).

The following equation:

$$\Xi_S(x,W) = \frac{\sinh(W\varphi)}{\sinh[(W+1)\varphi]} = 1 \tag{A18}$$

in terms of φ, has a purely imaginary solution, $\varphi = \frac{\pi \mathrm{i}}{2W+1}$, where $i = \sqrt{-1}$. Hence,

$$\frac{1 - z_S x}{(z_V - z_S)x} + \sqrt{\frac{(1 - z_S x)^2}{(z_V - z_S)^2 x^2} - 1} = \exp\left(\frac{\pi \mathrm{i}}{2W+1}\right) \tag{A19}$$

and

$$x = \frac{1}{z_S + (z_V - z_S)\cos\frac{\pi}{2W+1}}. \tag{A20}$$

To obtain a solution of Eq. (A17), x should be substituted by q/z_V and we get

$$q_c = \frac{z_V}{z_S + (z_v - z_S)\cos\frac{2\pi}{2W+1}} = \frac{1}{1 - a + a\,\cos\frac{\pi}{2W+1}}$$

or

$$U_c = -\ln\left(1 - a + a\,\cos\frac{\pi}{2W+1}\right), \tag{A21}$$

where $a = (z_V - z_S)/z_V$ is the probability of making a step between layers (for simple cubic lattice $a = 1/3$). In the large W limit

$$U_c \approx \frac{a}{2}\left(\frac{\pi}{2W+1}\right)^2 = \frac{a}{8}\left(\frac{\pi}{W+\frac{1}{2}}\right)^2. \tag{A22}$$

3. Smallest singularity of the generating function $\Xi_S(x,W)$

It is also instructive to study singularities of the GF $\Xi_S(x,W)$ because this issue is related to the problem similar to that studied in the present paper. Namely the smallest singularity of $\Xi_S(x,W)$ gives us the free energy of a macromolecule localized in a narrow slit of width W. (Note that the "full" GF of the macromolecule in the slit does not reduce, strictly speaking, to the GF of loops; but these two functions do have the same smallest singularity.)

From Eq. (12) it is clear that the desired singularity of $\Xi_S(x,W)$ is associated with the smallest root of the denominator on the right-hand side: $\sinh[(W+1)\varphi] = 0$. Again, in terms of φ, this equation has a purely imaginary solution, $\varphi = i\frac{\pi}{W+1}$. By expressing φ in terms of x, Eq. (A15), we obtain the smallest singularity of $\Xi_S(x,W)$,

$$x_c = \frac{1}{z_S + (z_V - z_S)\cos\frac{\pi}{W+1}}. \tag{A23}$$

When a macromolecule is put in the slit, it loses entropy as compared to the bulk. On the other hand, if the macromolecule gains an additional energy in the slit (for example, in the case when the slit if filled by the solvent, which is more preferential for the macromolecule than the bulk solvent), localization may be favorable. This may correspond, for example, to the following model system: A grafted macromolecule is put in the slit filled by a preferential solvent. There is a narrow hole in the wall which is impenetrable for slit and bulk solvents but the macromolecule can penetrate through this pore. (Note that we do not consider here kinetic aspects of this problem, like the time necessary for the chain to escape through the narrow pore and so on.)

If a monomer acquires a negative energy, $-U$, corresponding to an additional statistical weight $q = e^U$, the bulk-to-slit transition occurs if $u/z_V = x_c$, where $x_c$is given by the above formula. From this we obtain the expression for the critical adsorption energy U_c,

$$U_c = -\ln\left(1 - a + a\,\cos\frac{\pi}{W+1}\right). \tag{A24}$$

In the large-W limit,

$$U_c \approx \frac{a}{2}\left(\frac{\pi}{W+1}\right)^2. \tag{A25}$$

[1] R. Sinha, H. L. Frisch, and F. R. Eirich, J. Chem. Phys. **57**, 584 (1953).

[2] G. J. Fleer, M. A. Cohen Stuart, J. M. H. M. Scheutjens, T. Cosgrove, and B. Vincent, *Polymers at Interfaces* (Chapman & Hall, London, 1993).

[3] L. I. Klushin and A. M. Skvortsov, J. Phys. A: Math. Theory **44**, 473001 (2011).

[4] E. Eisenriegler, *Polymers Near Surfaces* (World Scientific, Singapore, 1993).

[5] R. J. Rubin, J. Chem. Phys. **43**, 2392 (1965).

[6] V. Privman and N. M. Švrakić, *Directerd Models of Interfaces., and Clusters: Scaling and Finite-Size Properties*, Lecture Notes in Physics (Springer-Verlag, Berlin, 1989).
[7] E. J. Janse van Rensburg, J. Phys. A: Math. Gen. **36**, R11 (2003).
[8] G. K. Iliev and E. J. Janse van Rensburg, J. Stat. Mech. (2011) P11013.
[9] T. M. Birshtein, E. B. Zhulina, and A. Skvortsov, Biopolymers **18**, 1179 (1979).
[10] A. M. Skvortsov, L. I. Klushin, G. J. Fleer, and F. A. M. Leermakers, J. Chem. Phys. **130**, 174704 (2009).
[11] M.-B. Luo, J. Chem. Phys. **128**, 044912 (2008).
[12] J. S. Klos, D. Romeis, and J.-U. Sommer, J. Chem. Phys. **132**, 024907 (2010).
[13] S. Bhattacharya, V. G. Rostiashvili, A. Milchev, and T. A. Vilgis, Macromolecules **42**, 2236 (2009).
[14] S. Bhattacharya, V. G. Rostiashvili, A. Milchev, and T. A. Vilgis, Phys. Rev. E **79**, 030802(R) (2009).
[15] S. Bhattacharya, H.-P. Hsu, A. Milchev, V. G. Rostiashvili, and T. A. Vilgis, Macromolecules **41**, 2920 (2008).
[16] S. Metzger, M. Müller, K. Binder, and J. Baschnagel, Macromol. Theory Simul. **11**, 985 (2002).
[17] T. Kreer, S. Metzger, M. Müller, K. Binder, and J. Baschnagel, J. Chem. Phys. **120**, 4012 (2004).
[18] Y. Lépine and A. Caillé, Can. J. Phys. **56**, 403 (1978).
[19] E. Eisenriegler, K. Kremer, and K. Binder, J. Chem. Phys. **77**, 6296 (1982).
[20] P.-G. de Gennes, *Scaling Concepts in Polymer Physics* (Cornell University Press, Ithaca, NY, 1979).
[21] P.-G. de Gennes, J. Phys. (France) **37**, 1445 (1976).
[22] A. A. Gorbunov and A. M. Skvortsov, Adv. Coll. Int. Sci. **62**, 31 (1995).
[23] H. N. W. Lekkerkerker and R. Tuinier, *Cooloids and the Depletion Interaction*, Lecture Notes in Physics (Springer, Berlin, 2011).
[24] A. A. Gorbunov, A. M. Skvortsov, J. van Male, and G. J. Fleer, J. Chem. Phys. **114**, 5366 (2001).
[25] A. Y. Grosberg and A. R. Khokhlov, *Statistical Physics of Macromolecues* (AIP Press, New York, 1994).
[26] L. D. Landau and L. M. Lifshitz, *Quantum Mechanics: Non-Relativistic Theory*, 3rd ed., Vol. 3 (Pergamon Press, London, 1977).
[27] T. M. Birshtein, Macromolecules **16**, 45 (1983).
[28] R. J. Rubin, J. Res. Natl. Bur. Stand. Sec. B **69**, 301 (1965).
[29] R. J. Rubin, J. Res. Natl. Bur. Stand. Sec. B **70**, 237 (1966).
[30] P. Grassberger, Phys. Rev. E **56**, 3682 (1997).
[31] H.-P. Hsu and P. Grassberger, J. Stat. Phys. **144**, 597 (2011).
[32] I. Teraoka, P. Cifra, and Y. Wang, Macromolecules **34**, 7121 (2001).
[33] D. I. Dimitrov, A. Milchev, K. Binder, L. I. Klushin, and A. Skvortsov, J. Chem. Phys. **128**, 234902 (2008).
[34] J. Krawczyk, I. Jensen, A. L. Owczarek, and S. Kumar, Phys. Rev. E **79**, 031912 (2009).
[35] E. J. Janse van Rensburg and A. R. Rechnitzer, J. Phys. A: Math. Gen. **37**, 6875 (2004).
[36] P. Grassberger, J. Phys. A: Math. Gen. **38**, 323 (2005).
[37] M. N. Barber, A. J. Guttman, K. M. Middlemiss, G. M. Torrie, and S. G. Whittington, J. Phys. A **11**, 1833 (1978).
[38] H. W. Diehl and S. Dietrich, Phys. Rev. B **24**, 2878 (1981).
[39] H. W. Diehl and M. Shpot, Nucl. Phys. B **528**, 595 (1998).
[40] C. Domb and M. S. Green (eds.), *Phase Transitions and Critical Phenomena*, Vol. 6 (Academic, London, 1976).
[41] R. Descas, J.-U. Sommer, and A. Blumen, J. Chem. Phys. **120**, 8831 (2004).
[42] R. Descas, J.-U. Sommer, and A. Blumen, Macromol. Theory Simul. **17**, 429 (2008).
[43] R. Hegger and P. Grassberger, J. Phys. A: Math. Gen. **27**, 4069 (1994).
[44] L. Schäfer (ed.), *Excluded Volume Effects in Polymer Solutions as Explained by the Renormalization Group* (Springer, Berlin, 1999).
[45] J. C. Le Guillou and J. Zinn-Justin, Phys. Rev. B **21**, 3976 (1980).
[46] P. Flajolet and R. Sedgewick, *Analytic Combinatorics* (Cambridge University Press, Cambridge, UK, 2009).
[47] C. A. J. Hoeve, E. A. DiMarzio, and P. Peyser, J. Chem. Phys. **42**, 2558 (1965).
[48] W. B. Jones and W. J. Thron, *Continued Fractions: Analytic Theory and Applications*: *Encyclopedia of Mathematics and Its Applications* (Addison-Wesley, Reading, MA, 1980).